HHS Public Access

Author manuscript

*Ultrasound Med Biol*. Author manuscript; available in PMC 2018 September 12.

Published in final edited form as:

*Ultrasound Med Biol*. 2018 September ; 44(9): 1996–2008. doi:10.1016/j.ultrasmedbio.2018.05.010.

# INACTIVATION OF PLANKTONIC *ESCHERICHIA COLI* BY FOCUSED 1-MHZ ULTRASOUND PULSES WITH SHOCKS: EFFICACY AND KINETICS UPON VOLUME SCALE-UP

**Andrew A. Brayman**[*], **Brian E. MacConaghy**[*], **Yak-Nam Wang**[*], **Keith T. Chan**[†], **Wayne L. Monsky**[‡], **Valery P. Chernikov**[§], **Sergey V. Buravkov**[¶], **Vera A. Khokhlova**[*,‖], and **Thomas J. Matula**[*]

[*]Center for Industrial and Medical Ultrasound, Applied Physics Laboratory, University of Washington, Seattle, WA, USA;

[†]Tacoma Radiology Associates, Tacoma WA, USA;

[‡]Department of Radiology, University of Washington, Seattle, WA, USA;

[§]Research Institute of Human Morphology, Laboratory of Cell Pathology, Moscow, Russia;

[¶]Faculty of Fundamental Medicine, M.V. Lomonosov Moscow State University, Moscow, Russia;

[‖]Department of Acoustics, Physics Faculty, M.V. Lomonosov Moscow State University, Moscow, Russia

## Abstract

This study addresses inactivation of *E. coli* in either 5- or 10-mL volumes, which were 50- to 100-fold greater than used in an earlier study (Brayman et al. 2017). Cells were treated with 1-MHz pulsed high-intensity focused ultrasound (10 cycles, 2-kHz repetition frequency, +65/−12.8 MPa focal pressures). The surviving fraction was assessed by coliform assay, and inactivation demonstrated curvilinear kinetics. The reduction of surviving fraction to 50% required 2.5 or 6 min in 5- or 10-mL samples, respectively. Exposure of 5 mL for 20 min reduced the surviving fraction to ~1%; a similar exposure of 10-mL samples reduced the surviving fraction to ~10%. Surviving cells from 5-min exposures appeared normal under light microscopy, with minimal debris; after 20 min, debris dominated. Transmission electron microscopy images of insonated samples showed some undamaged cells, a few damaged but largely intact cells and comminuted debris. Cellular damage associated with substantive but incomplete levels of inactivation can be variable, ranging from membrane holes tens of nanometers in diameter to nearly complete comminution.

### Keywords

Acoustic bacterial inactivation; *Escherichia coli* inactivation; Focused ultrasound; Pulsed HIFU; Light microscopy of bacterial HIFU lysate; Non-linear waveform distortion; Planktonic bacterial inactivation; Shock fronts; TEM of bacterial HIFU lysate; Ultrasonic bacterial inactivation

Address correspondence to: Andrew A. Brayman, Applied Physics Laboratory, 1013 N.E. 40th Street, Seattle WA 98105-6698 USA. mailbrayman@apl.washington.edu.

## INTRODUCTION

In a paper published recently, an overview was provided of primary publications and review articles dealing with acoustic inactivation of bacteria (Brayman et al. 2017), a topic of interest in a variety of fields, ranging from food preservation to medicine. One interest is in the potential use of high-intensity focused ultrasound (HIFU) to disinfect abscesses, which are walled-off, fluid-filled collections of pus. Our previous study involved *in vitro* benchtop experiments with *Escherichia coli* (*E. coli*), which provided a preliminary understanding of treatment parameters required for efficacy and of the kinetics of the effect. However, very small volumes were used (100 μL), and the ability to scale up the treatments to larger volumes was not determined. Moreover, there were exposimetric uncertainties caused by the use of very small volumes, resulting in active mixing at the fluid-air interface, a condition that may not occur in actual abscesses. The objective of the present study was to scale up the treatment volume as a preliminary but necessary step in progressing toward animal studies.

Bacterial inactivation by intense ultrasound results from inertial cavitation, either *via* direct mechanical effects related to the shear forces associated with bubble collapse (Gao et al. 2014) or *via* sonochemical effects (Joyce et al. 2003). Our earlier results obtained with *E. coli* are consistent with this general conclusion (Brayman et al. 2017). However, attempts to correlate bacterial inactivation with quantitative measurements of inertial cavitation activity have shown a relatively weak relationship (Vollmer et al. 1998); it is thought that confounding factors influenced this outcome. Although it has been argued that sonochemical production is not the principal mechanism responsible for acoustic microbe inactivation (Hua and Thompson 2000), it appears that both mechanical and sonochemical effects are involved in the lysis of gram-negative *E. coli* and gram-positive *Streptococcus mutans* by 0.5-MHz ultrasound *in vitro*, as evidenced respectively by empty bacterial shells seen on electron microscopy (Chandler et al. 2001), and by diminution of the cell inactivation effect by inclusion of a free radical scavenger (Koda et al. 2009).

The long-range goal of the research presented here is to develop non-invasive acoustic treatments to inactivate bacteria and other pathogens contained within the abscesses *via* cavitation. The overarching hypothesis, *viz.*, that cavitation fields can significantly reduce bacterial cell viability, has been well established, as described earlier in this report, and is not the focus of this paper. Instead, this study expands on the previous low-volume study, to test the specific hypothesis that HIFU-induced inactivation of bacteria in substantially larger volumes of 5 or 10 mL can be achieved rapidly and effectively. The volumes used here are up to two orders of magnitude larger than those used in the previous study. Parenthetically, abscesses of 10 mL have been characterized medically as large (Herzon 1985), although they can be much larger still.

The present study also overcomes some of the technical limitations from the previous work. In particular, a new exposure system was designed so that the acoustic focal volume was entirely within the sample volume. Furthermore, in contrast to our earlier study, there was little to no perturbation of the air—water interface. *De novo* cavitation was initiated within the sample volume; this was observable macroscopically when the HIFU was initiated.

Finally, the appearance of bacteria withdrawn from 5- or 10-mL sample volumes and subjected to either 0, 5 or 20 min of HIFU exposure was examined using both conventional light- and transmission electron microscopy (TEM). Although not tested statistically, our *a priori* expectation was that similar efficacy and similar kinetics could be achieved in these larger volumes. This expectation was met broadly. However, the kinetics changed, with the inactivation process occurring more slowly as volume increased.

## METHODS

### Culture and preparation

The biological materials and methods used here have been described in detail in our earlier paper (Brayman et al. 2017), except as noted. *E. coli* was selected as the test organism because it is a common inhabitant of abdominal abscesses, and *E. coli*-specific colony-forming plates are commercially available. Briefly, cell concentrations in liquid culture were estimated turbidometrically; the fraction of cells surviving the various treatments was determined by plating and colony counts. When liquid tryptic soy broth cultures had reached a cell concentration of about $1\times10^9$ cells/mL, the cultures were removed from the incubator and allowed to stand at room temperature. Then 5- or 10-mL aliquots were removed and transferred to the corresponding exposure vessel, which differed between the two volumes, as will be discussed later in this report. Sonications of the exposure vessels were conducted starting from room temperature initial conditions (~21°–C 23°C). This was used to avoid overheating of samples during the treatment and to minimize concentration changes and potential starvation effects in the *E. coli* stock suspension, were they to continue to incubate at 37°C, as will be discussed later. After HIFU exposure or no exposure, the surviving fraction (SF) of cells was determined by plating and colony counts.

### Acoustic system

A 44.5-mm diameter, spherically focused single-element transducer (F-number = 1) operating at 1.057-MHz resonance frequency was used. The transducer was mounted to a cylindrical tank filled with degassed water (Fig. 1). Calibration of the acoustic field was performed in water with a fiber optic probe hydrophone (FOPH 2000; RP Acoustics, Leutenbach, Germany; 100 $\mu$m active diameter, 100-MHz bandwidth). For this, the sample holder was removed.

The focus was determined as follows: A cavitation field in normal un-degassed water was generated, using a few cycles at high power. Fiducial marks were then placed at four locations around the tank, in line with the visible cavitation field to aid with initial alignment of the hydrophone. The water was then degassed with a vacuum pump and stir bar for 15 min, and the hydro-phone was placed near the center of the fiducial marks. It was then translated, using micrometer translation stages, until the peak positive pressure was found.

Pressure waveforms measured at the focus were deconvolved using the procedure provided by the hydro-phone manufacturer. To suppress the noise level of the hydrophone, single pulse measurements were averaged over 100 pulses. The pulses were aligned in time, relative to the position of the steep shocks developed in the focal waveforms at high source-

output levels, to compensate for the effects of phase jitter and corresponding broadening of the shocks and diminution of the peak positive pressure. This process of translating the hydrophone and waveform measurements was performed for each voltage level to generate a peak positive and peak negative pressure calibration (Fig. 2 a).

In further experiments of irradiating the bacteria, the transducer was driven at the highest peak voltage level of 265 $V_{p,}$ at which the free-field peak positive and negative pressures at the focus were +65 and −12.8 MPa, respectively. Under these conditions, the 10-cycle excitation of the transducer produced shock fronts in the acoustic waveform at the focus because of non-linear propagation effects (Fig. 2 b). The maximum shock amplitude in the single pulse measurements was equal to the maximum peak positive pressure, which corresponds to the level of non-linear waveform distortion, defined as a developed shock front (Rosnitskiy et al. 2015). As has been shown in recent studies, the peak pressure levels, which correspond to the formation of the developed shock, are mainly determined by the F-number of the transducer and are practically independent of its frequency or dimensions (Rosnitskiy et al. 2015, 2017). Indeed, the same peak pressures were measured for such waveforms in the field of transducers of the same dimensions but different frequency of 2 MHz (Canney et al. 2008) and of the same frequency and F-number but larger dimensions (Rosnitskiy et al. 2017).

## Exposure vessels

Two sizes of cylindrical plastic exposure vessels were used to accommodate the 5- or 10-mL samples (see Fig. 1 a and b). Both were ~48-mm long. The inside diameter of the 5-mL vessels was ~1.27 cm; that of the 10-mL vessels was ~1.91 cm. These diameter choices were made so that the height of the fluid column within the vessels would be similar (39 mm or 35 mm for 5-mL or 10-mL vessels, respectively, as measured from the lower membrane and neglecting the meniscus). Both vessels were fitted with a cling-film acoustic window held in place by an O-ring that nested in an annulus machined into the outer walls of the vessels (not shown in Fig. 1). After filling with the desired sample, the vessels were attached to a plastic positioning fixture of appropriate size. A small air gap was maintained between the fluid and the positioning fixture to avoid spillage of the bacterial suspension. The fixture was in turn attached to a 3-D motion stage. This allowed very reproducible alignment of replicate samples within the acoustic field.

## Treatment protocol

From our previous work, the peak negative pressure amplitude threshold for inactivation of *E. coli* at 2 MHz was more than 6 MPa (here we define inactivation as a *loss of colony-forming competence*, and not necessarily *immediate death* or *lysis*). Furthermore, there was an unambiguous increase in bacterial inactivation with increasing pressure amplitude above the threshold (*vide* Brayman et al. [2017], Fig. 4). To remove confounding effects from operating near the threshold, the study was performed at the highest voltage amplitude corresponding to peak positive and peak negative pressures of +65 and −12.8 MPa, respectively.

A single set of treatment parameters was used for all samples; only exposure duration differed. These were pulse length of 10 cycles; pulse repetition frequency (PRF) of 2 kHz and total treatment times of 0, 1, 2, 3, 5, 10 or 20 min. These variables were selected to be comparable with those used in our earlier study. An entire cycle through this series of treatment times was completed before replicating the series; there were four replicate series within an experiment. The degassed water was changed after each time point to reduce indirect heating of the specimens. Three replicate experiments were conducted on three different days.

After acoustic treatment, the vessels were removed, and a sample was taken for dilution and plating. The sample holder components were decontaminated before reassembly and re-use. This was accomplished by immersion with agitation for at least 1 min in 8.25% NaOCl, followed by flushing with water, immersion with agitation in 5% acetic acid to remove residual NaOCl, another water flush, similar treatment in 10% W:V $NaHCO_3$ to neutralize residual acetic acid, a last water flush and drying. Bacterial carryover was undetectable after the disinfection protocol.

## Viability assessment

Samples withdrawn from the treated cell suspensions were subjected to three serial dilutions with EPA dilution water (2 mM $MgCl_2$, 0.6 mM $KH_2PO_4$, pH 7.1) as a standard diluent for *E. coli* (United States Environmental Protection Agency Office of Water 2009), using aliquots no smaller than 25 μL and a total dilution factor of $6.774 \times 10^6$. This consistently produced the desired result of ~100–150 CFU/assay plate in the unexposed treatment groups. We placed 1 mL of the final dilution on the surface of Compact Dry EC100 assay plates (Hardy Diagnostics, Santa Maria, CA, USA), on which *E. coli* specifically produces a blue colony and other, non-*E. coli*, coliforms produce red colonies. Colonies were counted after incubation at 37°C for ~18 h, at which time the colonies were visible macroscopically. In most experiments, the plates were scored manually without blinding. However, in supplemental experiments, to ascertain the effects of temperature and potential cytotoxic chemical effects on cell viability (discussed later in this report), because of the large number of samples, the plates were scored using image analysis. Digitized images of the plates were classified and counted, using the advanced trainable Weka segmentation in the Fiji distribution of ImageJ (National Institutes of Health, Bethesda, MD, USA) and the particle analyzer plugin. Briefly, after Weka segmentation, the resulting binary images were thresholded and a watershed was applied to separate touching colonies. The particle analyzer was applied to the resulting image to obtain the CFU counts.

## Sample preparation for light or transmission electron microscopy

For light microscopy and for initial TEM fixation, HIFU-exposed or unexposed bacterial samples were fixed with half-strength Karnovsky's fixative. A drop of the fixed suspension was applied onto a polylysine-coated histologic slide, air-dried and then stained using the standard Romanovsky-Giemsa procedure. Image acquisitions were carried out under oil immersion, using a Zeiss upright microscope with 100 × objective (total magnification 1500 ×) and with an AxioCam MRc 5 megapixel camera.

For transmission electron microscopy (TEM), treated or unexposed bacteria were concentrated by centrifugation at 8,000 g × 20 min, and the supernatant was discarded. Pelleted fixed cells were treated with 1% osmium tetroxide solution for 30 min and dehydrated in a progressive series of ethanolic solutions (30%, 50%, 70% and 100%). After routine procedures, the pellets were stained with 1% uranyl acetate in 70% ethanol during dehydration and then embedded into epon-araldite. Ultrathin sections (70 100 nm) were then obtained on an LKB-III ultra-microtome (Mariehäll, Sweden). The sections were further contrasted with Reynolds lead cit-rate solution. Images were captured using a transmission electron microscope JEOL 1011 (Tokyo, Japan), equipped with a Gatan camera.

## RESULTS

### Macroscopic observations

During all exposure treatments, there was minimal agitation at the air-sample interface because of acoustic streaming; typically, a small hump formed at the interface. Neither visible droplet spray nor mist formed above the sample. Cavitation fields induced vigorous fluid mixing. Visible turbidity of the suspensions diminished as treatment time progressed.

### Acoustic heating

Post-treatment sample temperature was measured by inserting a small-gauge thermocouple into the sample fluid within 30 sec after removal from the water bath and dismounting the sample vessel from the plastic positioning fixture. As shown in Figure 3, the sample temperature increased in a curvilinear fashion, rising rapidly during the first 4 5 min and more slowly thereafter. The heating rate in the 5-mL samples was lower than with 10-mL samples, but the overall kinetics were similar between the two sample sizes. Possible reasons for this seemingly counter-intuitive result are discussed later in this report.

We estimated the temperature measurement error by measuring how quickly the temperature of hot water would decrease from an initial value of 50°C over 30 s, when poured into room-temperature exposure vessels in air; the temperature decreased by only 3°C. The error estimate can be considered as a worst-case scenario because our measurements were taken in less than 30 s, and, during actual treatment, the coupling water warmed slightly. Thus, the temperature difference between the vessel wall and vessel contents—and therefore heat diffusion rates—were lower in the actual experiments. The viability of *E. coli* at an elevated temperature is discussed later in this report.

### Effect of acoustic treatments on *E. coli* viability

Inactivation of *E. coli* was dependent strongly on total treatment time (Fig. 4), as has been observed by others under different specific conditions (vide [Brayman et al. 2017]). In previous experiments involving 100-mL volumes, the decline in the SF with increasing total exposure time was well described ($r^2 = 0.897$) as a half-life phenomenon, with a half-life of 1.2 min, as fit by the Eadie-Hofstee method (Eadie 1942; Hofstee 1959). In the present experiments, the kinetics are less clear-cut (Fig. 4). When 5-mL volumes were insonated at low exposure times, the decline in the SF appeared on the first inspection to follow first-order kinetics, with a half-time of around 2–3 min [*i.e.*, only 2–3 times longer than required

to achieve the same level of inactivation when using 100-$\mu$L samples (Brayman et al. 2017)]. However, the overall fit had an $r^2$ value for a first order fit of 0.77, being only slightly superior to that for a simple linear fit ($r^2 = 0.68$). For 10-mL volumes, a simple linear fit better described the data than did a first-order kinetic fit ($r^2 = 0.87$ versus 0.02, respectively).

We found 50% inactivation of *E. coli* in 5- or 10-mL volumes after ~2.5 or 6 min, respectively. In the 5-mL samples, about 95% inactivation was achieved after 10 min of exposure, declining to nearly 0% after 20 min. In the 10-mL volumes, about 80% of the bacteria had been inactivated after 10 min of exposure; inactivation declined further to around 95% after 20 min of exposure. It should be emphasized that the transducer remained stationary during sample exposure; bacteria from outside the focal volume entered the focal volume by vigorous mixing because of cavitation activity.

### Light microscopic and TEM appearance of HIFU- or unexposed *E. coli*

The appearance of unexposed or HIFU-exposed *E. coli* under light microscopy is presented in Figure 5 for material drawn from 5-mL (Fig. 5 a–c) or 10-mL (Fig. 5 d–f) sample vessels. For bacteria in 5-mL vessels, unex-posed and exposed to HIFU for 5 min (Fig. 5 a and b), the stained materials appear to be intact cells, with little to no evidence of debris. Although this image is not intended to be quantitative, it is noteworthy that what appears to be a high level of cellular integrity was associated with almost 75% inactivation of bacteria as assessed by coliform competence. For bacteria exposed in the 5-mL volume to HIFU for 20 min (Fig. 5 c), the optical field appears to be populated exclusively by stained cellular debris. Bacterial inactivation under these conditions was >99.5%.

For bacteria in the 10-mL vessels, unexposed (Fig. 5 d) and exposed to HIFU for 5 min (Fig. 5 e), like the 5-mL samples, the cells appear to be intact and there is no evidence of comminuted debris. However, the staining pattern for the 5-min exposure is heterogeneous. We found that 50% of the cells associated with this exposure treatment were inactivated. Figure 5 (f) shows bacteria exposed to HIFU in the 10-mL volume for 20 min. Evident in this image are many apparently intact cells, with a background of comminuted debris. The cell inactivation associated with this treatment was about 95%, as measured by the plating efficiency.

These results show that inactivated bacteria may still appear normal under optical microscopy. TEM was used for higher resolution examination of structural damage to the treated bacteria. Figures 6–10 present the appearance of bacteria drawn from 5-mL or 10-mL samples that were either unexposed or exposed to HIFU for either 5 or 20 min.

Figure 6 shows the TEM of unexposed *E. coli* at various magnifications. Different shapes of the bacteria, varying from spherical to elongated rod-shaped, depending on the cell cycle and their orientation in section, are presented in an overview image (Fig. 6 a); many of the cells appear to be in the division stage. Thick cell walls of high or low contrast, regions of high and low electron density and two newly divided cells (*arrows*) are visible in the middle-magnification view (Fig. 6 b). The bacterial cytoplasm is electron dense, but populated with regions of lower electron density largely associated with the cell membrane. The cells in the high-magnification view (Fig. 6 c) appear to be intact with no obvious damage to the inner

or outer cell membranes as well; the appearance of the low-contrast thick wall of bacteria that possibly corresponds to pili on the bacteria surfaces is indicated by an arrow.

Figure 7 shows TEM images of cells treated in 5-mL volumes for 5 min. A mixture of obviously broken or empty cells missing cytoplasm, cell wall fragments, disorganized cytoplasmic debris and some visually intact cells is visible (Fig. 7 a). Three apparently intact cells share the optical field in Figure 7 (b) with three damaged cells and many cellular fragments. At a higher magnification (Fig. 7 c) of the optical field of view in Figure 7 (b), characteristic cell conditions are clearly visualized: An electron-dense cell essentially indistinguishable from the unexposed cells (Fig. 6); a cell in which the cell wall appears intact, but the cell is almost free of cytoplasm; and a cell with an approximately 120-nm hole formed in the cell wall. No low-contrast bacteria walls are visible (*i.e.*, the pili on the bacteria surface appear to have been lost). The coliform assay showed ~75% of the cells were inactivated by the 5-mL volume, 5-min exposure treatment combination.

Significantly stronger damage to the cells treated for 20 min in a 5-mL volume is demonstrated by TEM in Figure 8. The cells in the overview image (Fig. 8 a) appear damaged, with no signs of cytoplasm visible inside the cells; destroyed cell walls; and vesicular bodies seen in the cell remnants. Empty cell walls and fragments populate the optical field at a higher magnification (Fig. 8, b). At the highest magnification, (Fig. 8 c), a hole in the bacterial cell wall (*arrow*) is obvious. It cannot be determined whether this hole was larger at some location out of this plane of section, but as measured in this image, the hole diameter was 35 nm. The cell is essentially devoid of cytoplasm. As measured by coliform assay, more than 99% of the bacterial cells were inactivated by the 5-mL volume, 20-min exposure treatment combination.

Figure 9 shows TEM images of the cells treated in 10-mL volumes for 5 min. As shown in the overview image (Fig. 9 a), contrary to the same exposure of the 5-mL sample, the number of visually intact cells here dominates the number of obviously damaged cells, with a partial or almost entire loss of cytoplasm. Higher-magnification views show damaged cells with a vacuolated appearance (Fig. 9 b) and a cell with an invaginated region of its wall (Fig. 9 c, *arrow*). Low-contrast thick walls are seen for some bacteria, indicating possible survival of pili on the surface of the bacteria. As measured by coliform assay, about 50% of the bacterial cells were inactivated by the 10-mL volume, 5-min exposure treatment combination.

TEM results for longer, the 20-min treatment of the 10-mL sample volume are shown in Figure 10. The cells appear as evidently damaged in the overview image (Fig. 10 a). At higher magnifications, cell fragments and cell remnants essentially devoid of cytoplasm are clearly evident (Fig. 10 b and c). Of interest is the gap in the wall of one cell (*arrow*) in Figure 10 (c); the diameter of this gap was measured to be 33 nm at this plane of section. This cell appears to have been ready to divide, as two new cell walls have been formed, and also to have experienced a significant loss of cytoplasmic contents. As measured by coliform assay, about 95% of the bacterial cells were inactivated by the 10-mL volume, 20-min exposure treatment combination.

## DISCUSSION

The present bench-scale study of bacterial cell inactivation of *E. coli* suspensions of ~1 × $10^9$ cells/mL by low duty-factor pulsed HIFU (Fig. 4) proceeded with approximately first-order rate kinetics when 5-mL volumes were insonated, as has been reported by others (Drakapoulou et al. 2009, Ugarte-Romero et al. 2007). Compared with our earlier, small-scale studies, in which a 50% inactivation benchmark was achieved in about 1.2 min when 0.1-mL volumes were insonated (at 2 MHz, using a different exposure configuration), here the 50% inactivation threshold was reached in only 2.5 min in the 5-mL sample volumes exposed to 1-MHz fields, as described here. Despite the differences in the exposure conditions between the two sets of experiments, it is encouraging from a systems development perspective that treatment of a volume 50-fold greater attained the same 50% level of inactivation after only about a twice longer treatment. We found that 20 min of treatment of the 5-mL samples inactivated more than 99% of the cells.

When 10-mL volumes were insonated, the kinetics of bacterial inactivation were nearly linear during the first 10 min of exposure, as has also been reported by others (Scherba et al. 1991). However, the initially rapid inactivation rates slowed between 10 and 20 min. Fifty percent bacterial inactivation required about 6 min in the 10-mL samples compared with the twice shorter time of about 3 min in the twice smaller volume of 5 mL. Again, neglecting the differences in exposure systems used between this study and our earlier one, it is notable that a 100-fold increase in treated volume required only a 5-fold increase in treatment time. However, even with 20 min of exposure, around 5% of the treated cells retained colony-forming competence. Note that the time of 20 min needed for 95% bacterial inactivation in the10-mL sample was also nearly twice longer than that of about 10 min needed for the twice smaller 5-mL sample. As bacterial inactivation presumably occurred in the focal volume of the beam and the exposure vessel contents were mixed because of acoustic streaming, a certain volumetric inactivation per time could be introduced for this particular system, which is 1.6 mL/min for 50% and 0.5 mL/min for 95% inactivation. Although not tested here, it is possible that the half-life and total counts would both decrease if the transducer focus was moved within the sample during insonation, rather than allowing the mixing to control the kinetics of when bacteria were in the acoustic beam.

On light microscopy (Fig. 5), cells treated in either 5-mL or 10-mL volumes for 5 min retained a normal appearance, even though the SF had been reduced to 0.26 ± 0.07 (SEM) or 0.51±0.06, respectively. After 20 min of exposure, cells in the 5-mL samples had been comminuted (SF = 0.004 ± 0.001). In the 10-mL samples, light microscopy of the samples treated for 20 min showed a mix of apparently intact cells and cellular debris. These results suggest that light microscopic appearance is not a useful predictor of whether insonified *E. coli* cells are or are not coliform competent (*i.e.*, that damage much more subtle than visible on light microscopy could produce large changes in the SF).

TEM images showed qualitatively similar results but provided deeper insight into the mechanisms of damaging the bacteria by ultrasound. With the 5-mL, 5-min treatment (Fig. 6), a mix of clearly damaged and some apparently undamaged cells were present; after longer, the 20-min treatment, (Fig. 7), essentially all the cells were destroyed and mostly

devoid of cytoplasm. In one case, a largely intact cell wall was observed to have been penetrated by a 35-nm diameter hole (Fig. 7 c). In the 10-mL, 5-min treatment (Fig. 8), about half of the observable cells appeared to be intact and filled with normal-looking electron-dense cytoplasm, with the other half having lost significant (and presumably lethal) amounts of cytoplasm. After longer, 20-min treatments, the bacterial cells appear to have been almost entirely comminuted (Fig. 9), although the SF was about 5%. One apparently intact cell (Fig. 9 c), when viewed at very high magnification, had experienced subtle damage; *viz*, a hole of 33-nm diameter in the plane of the section that penetrated the inner and outer membranes.

The observed bioeffects were almost certainly mediated by inertial cavitation, as evidenced by both the apparently biologically insignificant temperature rise observed in the insonated samples (discussed later in this report), and by the extensive mechanical disruption of the bacterial cells. The major mechanisms for cavitation-induced effects include shear (either during expansion or collapse of the bubble), jetting (a mechanical jet impacting the bacteria) or shock waves (from the original incident pressure waveform or inertial collapse of bubbles). Some of these mechanisms have been observed in *ex vivo* vessels (Chen et al. 2011, 2012). Although many of the inactivated cells were seen to be reduced to small fragments, the presence of very small holes in some of the bacterial membranes indicates that cell damage can be highly localized and of a very small scale. These holes are often thought to be associated with cavitation jets. That interpretation may be correct here as well, although it must be remembered that these cells experienced ultrasound exposure for many min, so the actual mechanism is unclear.

We hypothesize that several beneficial factors contributed to the substantial increase in the treatment efficacy of the current pulsed HIFU system. First, frequency reduction from 2 to 1 MHz resulted in enhanced cavitation and enlarged dimensions of the focal region. Second, the formation of shocks at the focus are conducive to the generation of a cavitation cloud because of backscattering of high-amplitude shocks from single cavitation bubbles. Such scattering leads to the generation of large negative pressures as the positive-pressure phase of the wave inverts on scattering and superimposes on the incident negative-pressure phase to initiate further cavitation bubbles, and thereby form a large cloud (Maxwell et al. 2011). Acoustic streaming and resultant fluid mixing is enhanced substantially in the presence of shocks, because of the enhanced absorption of ultra-sound energy and transfer of the momentum to the fluid. Moreover, the presence of steep shocks by itself may contribute to the mechanical damage of cells *via* the mechanism of shear stresses. The acoustic wavelength of 1.5 mm at 1 MHz in water is much larger than a characteristic size of a bacteria (1–2 $\mu$m). However, the width of a 60-MPa shock front balanced by non-linear and thermoviscous effects, and estimated using weak-shock theory, is about 0.15 $\mu$m (Perez et al. 2013), which is much less than the bacterial dimensions. Propagation of shocks through the volume of bacteria thus can result in inhomogeneous stress and strain distributions over their surface. One future comparison will be to determine whether the efficacy is maintained with high-amplitude, nonshocked waveforms.

Another potential factor we considered was whether leachates from the polycarbonate exposure vessels might be cytotoxic to the bacteria. Indeed, dental brackets made of

polycarbonate may or may not be cytotoxic, apparently depending strongly on the brand of the product (Kloukos et al. 2013; Pithon et al. 2009; Retamoso et al. 2012; Vitral et al. 2010). We performed a study to assess any apparent cytotoxicity related to our 10-mL industrial-grade polycarbonate exposure vessels. Bacterial suspensions were incubated in them at either room temperature or at 45°C in a temperature-controlled water bath for up to 20 min. These temperatures correspond, to within 3°C, to the initial and maximum temperatures reached during sonication. Colony-forming unit (CFU) counting was performed at 0, 10 or 20 min and compared with controls, which were samples withdrawn from the stock cell cultures at the time of sample loading into the vessels. No changes from the initial state CFU control counts were observed from within a single temperature, nor between the two temperature exposures (Fig. 11). The study showed that our sample holders are not cytotoxic, and also bacterial viability was not compromised by incubation at 45°C for 20 min.

Thermal effects may play a larger role in cell inactivation under physiologic conditions (*i.e.*, higher initial temperatures would result in higher final temperatures after insonation). There may be a synergistic effect of heating stresses and cavitation occurring in tandem, as these two insults delivered together may induce additional inactivation. Moreover, high temperature elevation may cause thermal denaturation effects, although it has been reported that a thermally induced 100% kill rate of *E. coli* requires 45 min at 60°C (Jenkens et al. 1988). Even in the present study, relatively mild thermal stress may have increased bacterial susceptibility to cavitation damage. The effect of temperature will be tested in more detail in future studies.

Our observations indicate that cells in the stock suspension continued to multiply on the benchtop, but the increase was small during the several hours of an experiment, as assessed by optical density measurements before and at the conclusion of some experiments. We conducted our experiments starting from a room temperature initial state because we were concerned that were we to have maintained the cells at 37°C throughout, they would begin to starve and change their biological state before the experiment had concluded. For example, starvation is known to confer reduced sensitivity to heat or chemical challenges in *E. coli* (Jenkens et al. 1988). This hypothesis was not tested in this study, as the main goal was to compare these scaled-up volumes to the earlier study.

Finally, the 5-mL or 10-mL samples experienced somewhat different heating rates, with the 10-mL samples heating to a few degrees higher than the smaller volume samples (Fig. 3). We presume that these small differences reflect a surface-to-volume ratio more conducive to heat exchange between the sample and the water bath in the 5-mL vessels (surface:volume ~3.4 $cm^{-1}$, versus ~2.4 $cm^{-1}$ in 10-mL vessels). Moreover, the larger vessels had significantly thicker walls than did the 5-mL vessels, which would also have impeded heat transfer.

## CONCLUSIONS

HIFU-induced inactivation of bacterial suspensions of controlled species and defined number concentration was scaled up successfully from the 100-$\mu$L volumes used in our

previous study, to volumes 50 or 100 times larger; *viz.*, 5 mL or 10 mL. Although the exposure system differed in several ways between the previous study and this one, the results are encouraging from the perspective of development of a treatment technology. The time course of the bacterial inactivation slowed as the sample volume increased, but in a highly non-linear way. With 0.1-mL samples, 50% inactivation required about 1.2 min (Brayman et al. 2017); with 5- or 10-mL samples, this state was achieved in 2.5 or 6 min, respectively. The treatments applied in the present experiment were therefore much more efficient at inactivating bacteria than were the previously used, low-volume experiments (Brayman et al. 2017). As a first-order approximation (*i.e.*, simplifying to linear rates of cell killing to inactivate 50% of the cells), inactivation rates were 42, 1000 or 833 million cells/min for the 0.1-, 5- or 10mL treatments, respectively.

## Acknowledgments—

This research was supported by NIH grants 5 R01 EB019365, 2 R01 EB007643 and by RFBR 16–02-00653. The authors thank the Electron Microscopy Laboratory of the Biological Faculty of Moscow State University for the help in TEM analysis and Dr. Richard P. Darveau of the Department of Periodontics, School of Dentistry, University of Washington, for critical reading of the manuscript and helpful discussions. The authors also thank the anonymous reviewers of the manuscript for constructive criticisms that strengthened the paper.

## REFERENCES

Brayman AA, MacConaghy BE, Wang Y-N, Chan KT, Monsky WL, McClenny AJ, Matula TJ. Inactivation of planktonic *Escherichia coli* by focused 2-MHz ultrasound. Ultrasound Med Biol 2017;43:1476–1485. [PubMed: 28454842]

Canney MS, Bailey MR, Crum LA, Khokhlova VA, Sapozhnikov OA. Acoustic characterization of high intensity focused ultrasound fields: A combined measurement and modeling approach. J Acoustic Soc Am 2008;124:2406–2420.

Chandler DP, Brown J, Bruckner-Lea CJ, Olson L, Posakony GJ, Stults JR, Valentine NB, Bond LJ. Continuous spore disruption using radially focused, high-frequency ultrasound. Anal Chem 2001;73:3784–3789. [PubMed: 11510849]

Chen C, Kreider W, Brayman AA, Bailey MR, Matula TJ. Blood vessel deformations on microsecond time scales by ultrasonic cavitation. Phys Rev Lett 2011;106 034301. [PubMed: 21405276]

Chen H, Brayman AA, Evan AP, Matula TJ. Preliminary observations on the spatial correlation between short-burst microbubble oscillations and vascular bioeffects. Ultrasound Med Biol 2012;38:2151–2162. [PubMed: 23069136]

Drakapoulou S, Terzakis S, Fountoulakis MS, Mantzavinos D, Manios T. Ultrasound-induced inactivation of gram-negative and gram-positive bacteria in secondary treated municipal wastewater. Ultrason Sonochem 2009;16 629–624.

Eadie G The inhibition of cholinesterase by physostigmine and pros-tigmine. J Biol Chem 1942;146:85–93.

Gao S, Lewis GD, Ashokkumar M, Hemar Y. Inactivation of microorganisms by low-frequency high-power ultrasound: 2. A simple model for the inactivation mechanism. Ultrason Sonochem 2014;21:454–460. [PubMed: 23845410]

Herzon FS. Management of nonperitoneal abscesses of the head and neck with needle aspiration. Laryngoscope 1985;95:780–781. [PubMed: 4010416]

Hofstee B Non-inverted versus inverted plots in enzyme kinetics. Nature 1959;184:1296–1298. [PubMed: 14402470]

Hua I, Thompson JE. Inactivation of *Escherichia coli* by sonication at discrete ultrasonic frequencies. Water Res 2000;34:3888–3893.

Jenkens D, Schultz J, Martin A. Starvation-indiced cross-protection against heat or $H_2$ $O_2$ challenge in *Escherichia coli*. J Bacteriol 1988;170:3910–3914. [PubMed: 3045081]

Joyce E, Phull SS, Lorimer JP, Mason TJ. The development and evaluation of ultrasound for the treatment of bacterial suspensions. A study of frequency, power and sonication time on cultured *Bacillus* species. Ultrason Sonochem 2003;10:315–318. [PubMed: 12927605]

Kloukos D, Taoufik E, Eliades T, Katsaros C, Eliades G. Cytotoxic effects of polycarbonate-based orthodontic brackets by activation of mitochondrial apoptotic mechanisms. Dental Mater 2013; 29e35–e44.

Koda S, Miyamoto M, Toma M, Matsuoka T, Maebayashi M. Inactivation of *Escherichia coli* and *Streptococcus mutans* by ultrasound at 500 kHz. Ultrason Sonochem 2009;16:655–659. [PubMed: 19282231]

Maxwell AD, Wang T-Y, Cain CA, Fowlkes JB, Sapozhnikov OA, Bailey MR, Xu Z. Cavitation clouds created by shock scattering from bubbles during histotripsy. J Acoustic Soc Am 2011;130:1888–1898.

Perez C, Chen H, Matula TJ, Karzova M, Khokhlova VA. Acoustic field characterization of the Duolith: Measurements and modeling of a clinical shock wave therapy device. J Acoustic Soc Am 2013;134:1663–1674.

Pithon MM, Santos RL, Martins FO, de Oliveira Ruelllas AC, Nojima LI, Nojima MG, Romanos MTV. Cytotoxicity of polycarbonate orthodontic brackets. Braz J Oral Sci 2009;8:84–87.

Retamoso LB, Luz TB, Marinowic DR, Machado DC, De Menezes LM, Freitas MP, Oshima HM. Cytotoxicity of esthetic, metallic, and nickel-free orthodontic brackets: Cellular behavior and cytotocity. Am J Orthod Dentofacial Orthoped 2012;142:70–74.

Rosnitskiy PB, Yuldashev PV, Khokhlova VA. Effect of the angular aperture of medical ultrasound transducers on the parameters of non-linear ultrasound field with shocks at the focus. Acoust Physics 2015;61:301–307.

Rosnitskiy PB, Yuldashev PV, Sapozhnikov OA, Maxwell AD, Kreider W, Bailey MR, Khokhlova VA. Design of HIFU transducers for generating specified non-linear ultrasound fields. IEEE Trans UFFC 2017;64:374–390.

Scherba G, Weigel RM, O'Brien WD, Jr.. Quantitative assessment of the germicidal efficacy of ultrasonic energy. Appl Environ Microbiol 1991;57:2079–2084. [PubMed: 1892396]

Ugarte-Romero E, Feng H, Martin SE. Inactivation of *Shigella boydii* 18 IDPH and Listeria *monocytogenes Scott* A with power ultra-sound at different acoustic energy densities and temperatures. J Food Sci 2007;72:M103–M107. [PubMed: 17995776]

United States Environmental Protection Agency Office of Water. Method 1603: *Escherichia coli* (*E. coli*) in water by membrane filtration using modified membrane-thermotolerant *Escherichia coli* agar (modified mTEC). 4Washington, DC: United States Environmental Protection Agency Office of Water (4303 T); 2009 Publication number EPA-821-R-09–007.

Vitral JC, Fraga MR, de Souza MA, Ferreira AP, Vitral RW. *In-vitro* study of cellular viability and nitric oxide production by J774 macrophages stimulated by interferon gamma with ceramic, polycarbonate, and polyoxymethylene brackets. Am J Orthodont Dentofacial Orthop 2010;137:665–670.

Vollmer AC, Kwakye S, Halpern M, Everbach EC. Bacterial stress responses to 1-megahertz pulsed ultrasound in the presence of microbubbles. Appl Environ Microbiol 1998;64:3927–3931. [PubMed: 9758821]

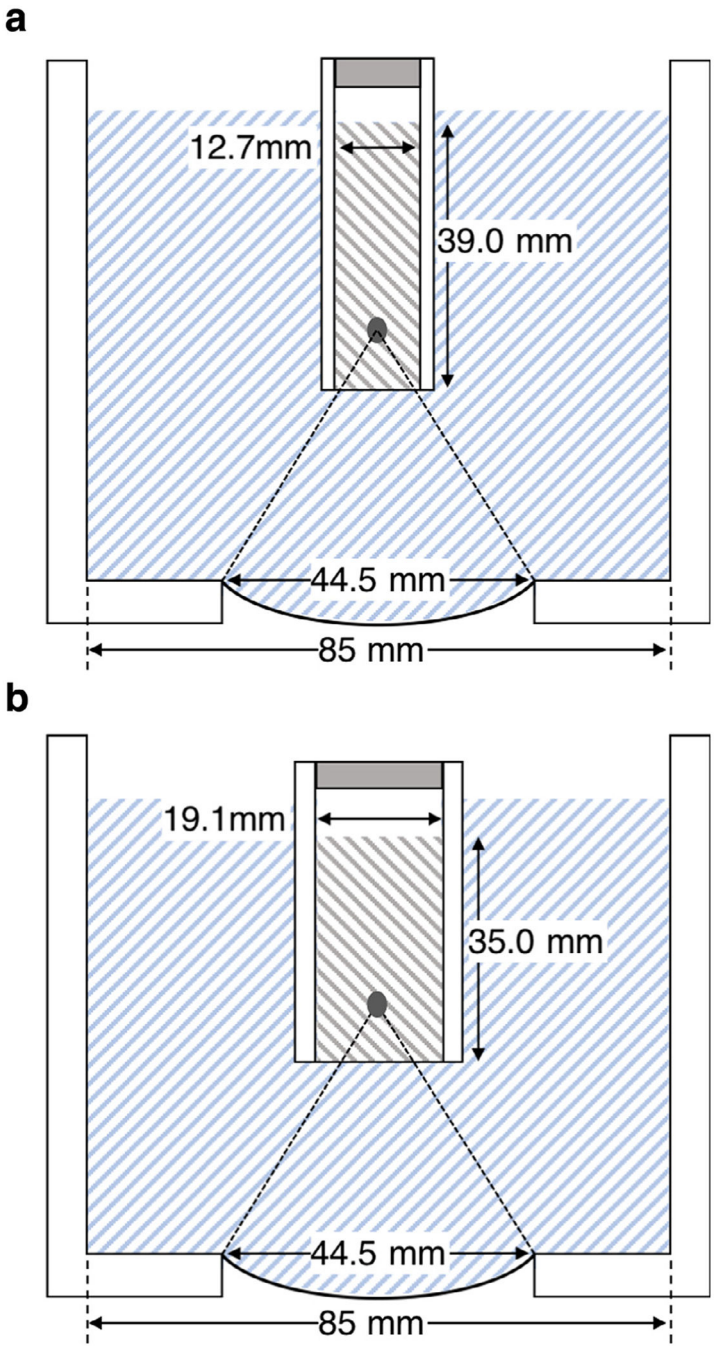


**Fig. 1.**

The transducer and water bath assembly for (a) 5-mL or (b) 10-mL samples. Although not strictly to scale, the location and size of the cavitation zone is approximately correct. A small air gap was left between the fixtures and the sample fluid to avoid displacing the bacterial suspensions when assembling the filled vessels.

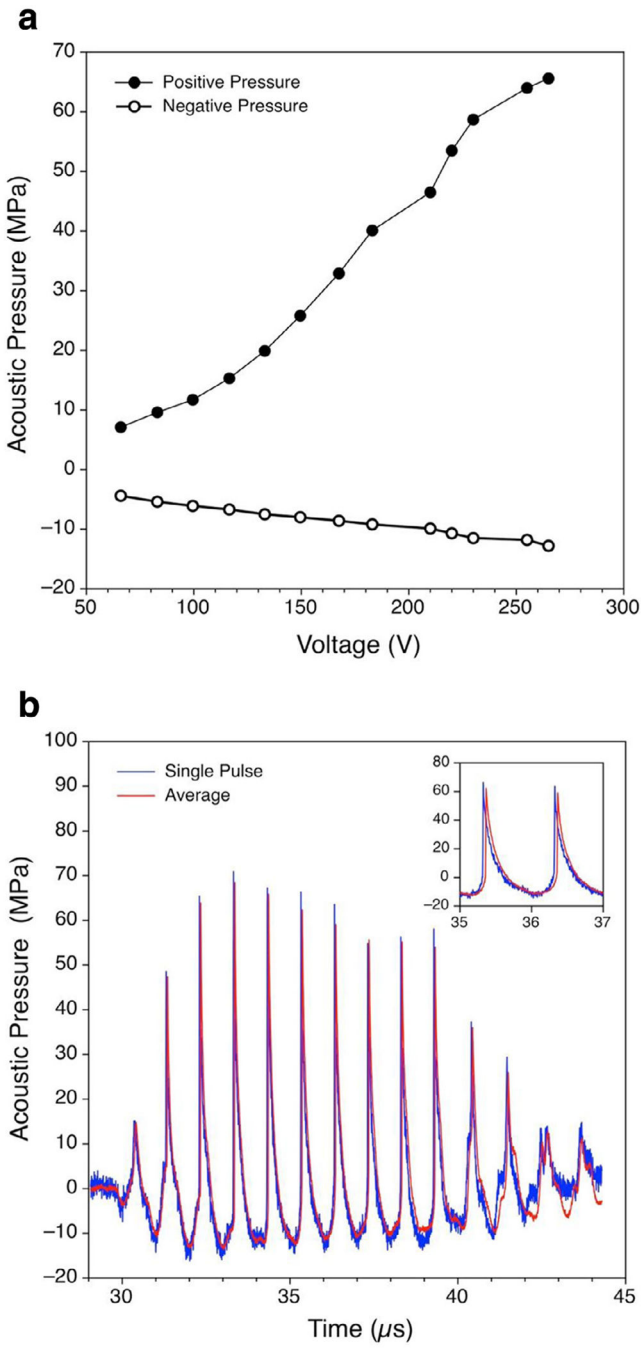


**Fig. 2.**

Acoustic characterization results. (a) Peak positive and peak negative pressures in acoustic waveforms measured by a fiber optic probe hydrophone at the focus in water versus peak driving voltage applied to the transducer. (b) Focal pressure waveforms (single pulse and averaged over 100 pulses) with a peak positive pressure of +65 MPa and a peak negative pressure of −12.8 MPa measured at the highest output level of 265 V peak, at which sonication of biological samples was performed. Note the presence of steep shock fronts up

to 65 MPa amplitude formed in the pulse waveform because of non-linear propagation effects.

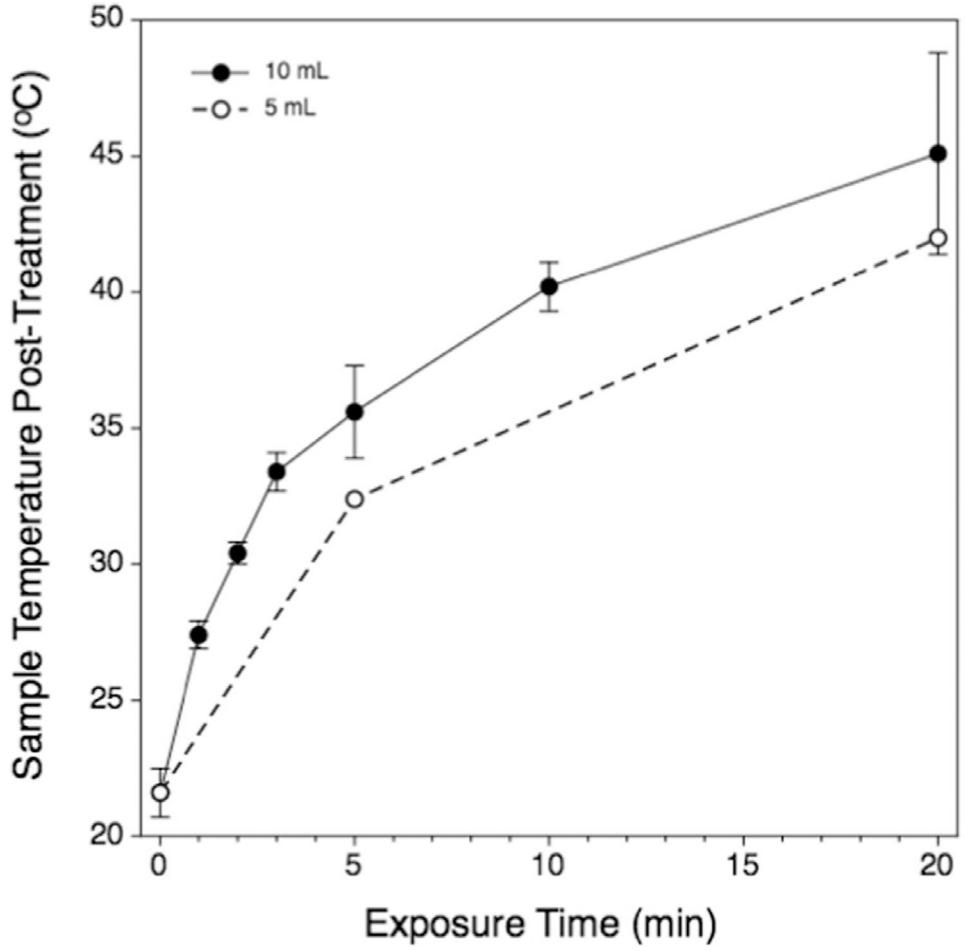


**Fig. 3.**

Time-temperature relationship for representative 5-mL samples (*open circles*) or 10-mL samples (*filled circles*). The heating kinetics was similar; however, the 10-mL samples were heated more rapidly than were the 5-mL samples and attained a slightly higher maximum temperature. Samples from both volumes were treated at the time points indicated for the 10-mL samples. Temperature data for the 5-mL samples were not as comprehensive as for the 10-mL groups.

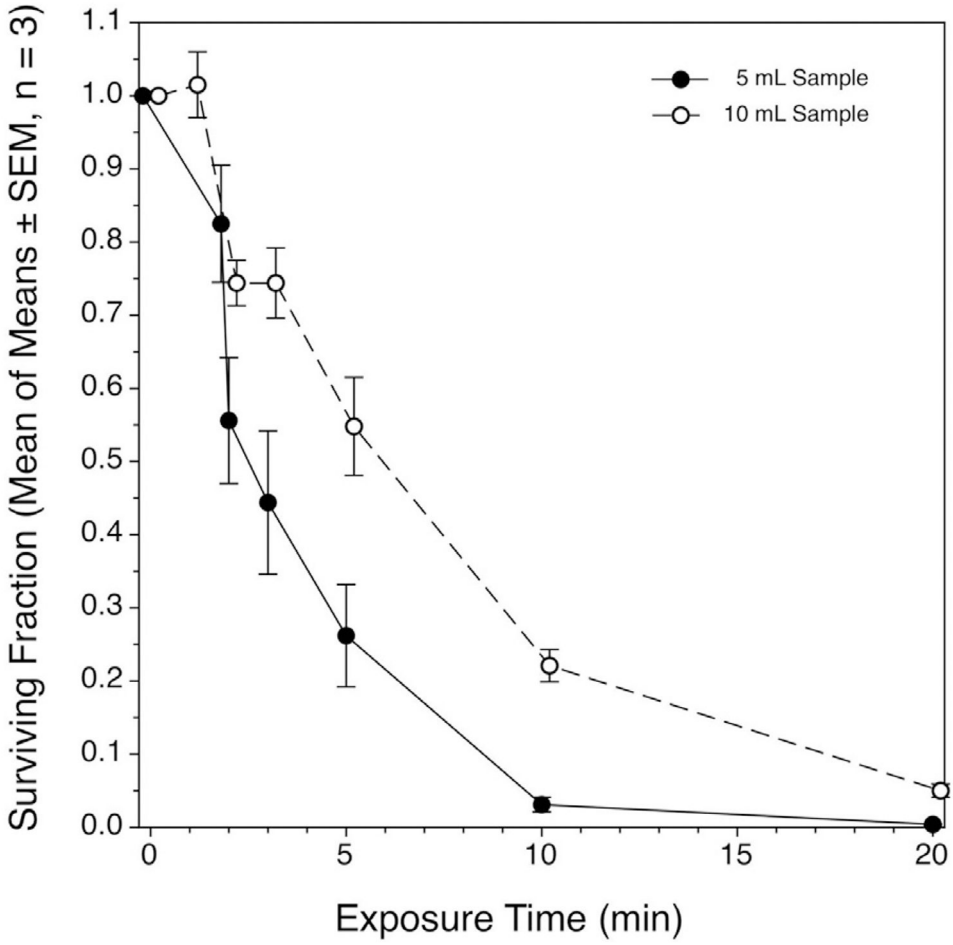


**Fig. 4.**

Recovery of coliform-competent *E. coli* cells suspended in 3% tryptic soy broth after high-intensity focused ultrasound treatment. Each of three replicate experiments per treated volume were made up of four replicate samples per time point within the experiment. The means of means of the SFs, ± the standard errors of the means are plotted. For both treated volumes, the decline in the SF was related to exposure time in curvilinear fashion, but in neither case were the data well described by first order kinetics.

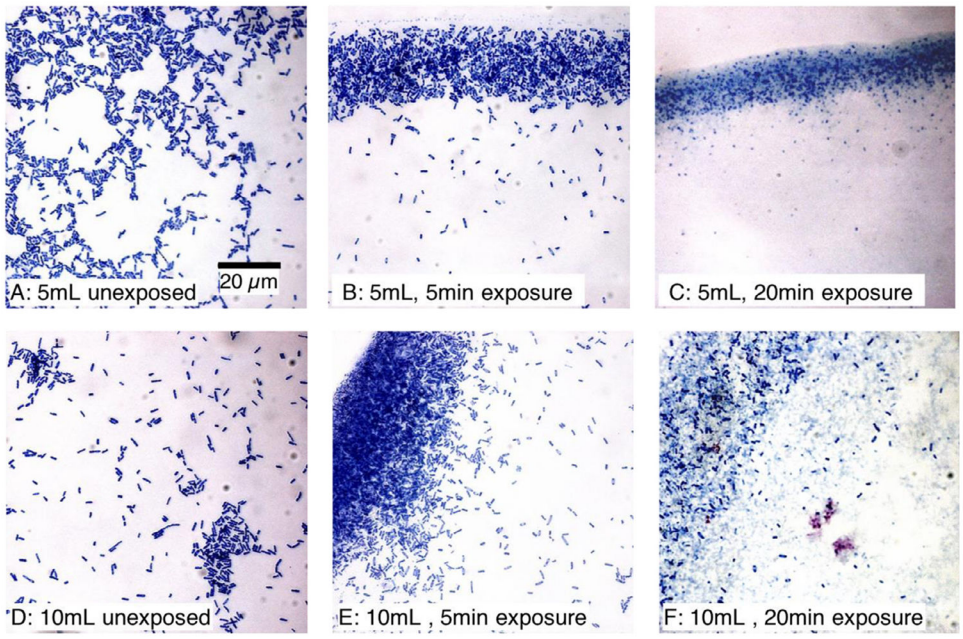


**Figure 5.**

Appearance of *E. coli* cells from 5-mL (a–c) or 10-mL (d–f) samples stained using the Romanovsky-Giemsa method. The images are not quantitative. (b, e) Material seems to be intact cells and cellular debris appears to be absent. However, the surviving fraction (SF) was (b) 0.26 ± 0.07, and (e) 0.51 ± 0.16. (c) Materials seem to be made up of cellular debris; SF at this exposure time was 0.004 ± 0.001. (f) Many apparently intact cells are visible. The associated SF was consistent with this observation, being 0.05±0.04 (*i.e.*, about 10-fold greater than in [c]).

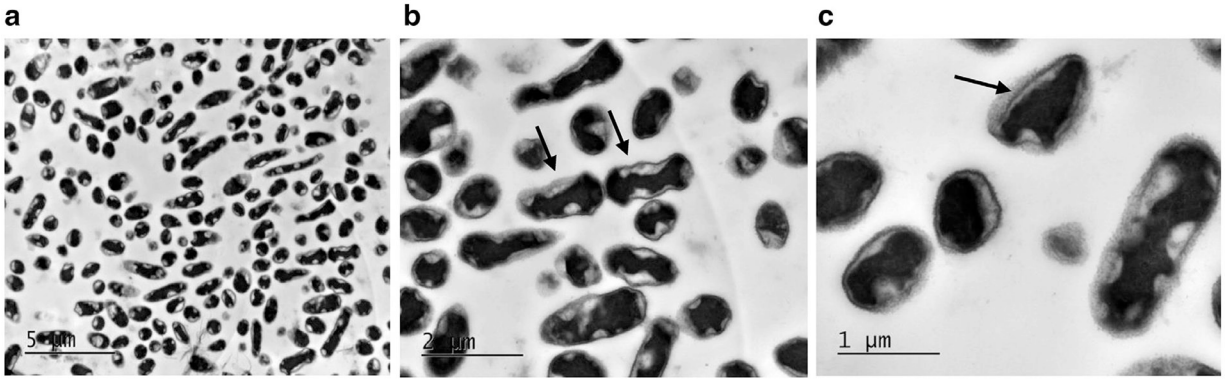


**Fig. 6.**

Transmission electron microscopy (TEM) appearance of unexposed *E. coli* cells at (a) the low magnification (8000 ×, scale bar is 5 $\mu$m), (b) the middle magnification (20,000 ×, scale bar is 2 $\mu$m) and (c) the high magnification (40,000 ×, scale bar is 1 $\mu$m). (a) Representative distribution of different shapes of the bacteria, varying from spherical to elongate rod-shaped, depending on the cell cycle and their orientation in TEM section. Two newly divided cells (*arrows*) and regions of high- and low-electron density are visible with the middle magnification (b) Pili on the surfaces of the bacteria (*arrow*) are resolved with high magnification (c). Although the images are not quantitative, the surviving fraction as measured by colony formation was 1.00 by definition.

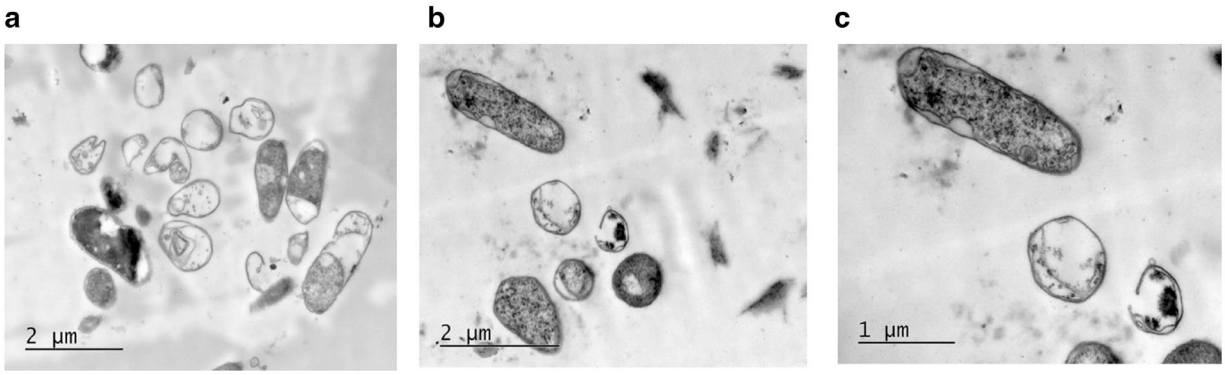


**Fig. 7.**

Transmission electron microscopy appearance of *E. coli* cells from the 5-mL, 5-min exposure treatment combination. At the low magnification (a) (20,000 ×, scale bar is 2 μm), nearly all cells are seen as damaged and missing cytoplasm to various extents; many cell wall fragments are evident. In another field of view (b) (25,000 ×, scale bar is 2 μm), three apparently intact cells share the optical field with three damaged cells and many cellular fragments. The high magnification view (c) (40,000 ×, scale bar is 1 μm) of a smaller portion of the optical field in (b) shows an electron-dense cell essentially indistinguishable from those in unexposed cell images (Fig. 6), a cell in which the cell wall in this plane of section appears intact but the cell is almost free of cytoplasm, and a cell in which an approximately 120-nm hole exists. No pili remain on the bacterial surfaces. The surviving fraction associated with this treatment combination was 0.26 ± 0.07.

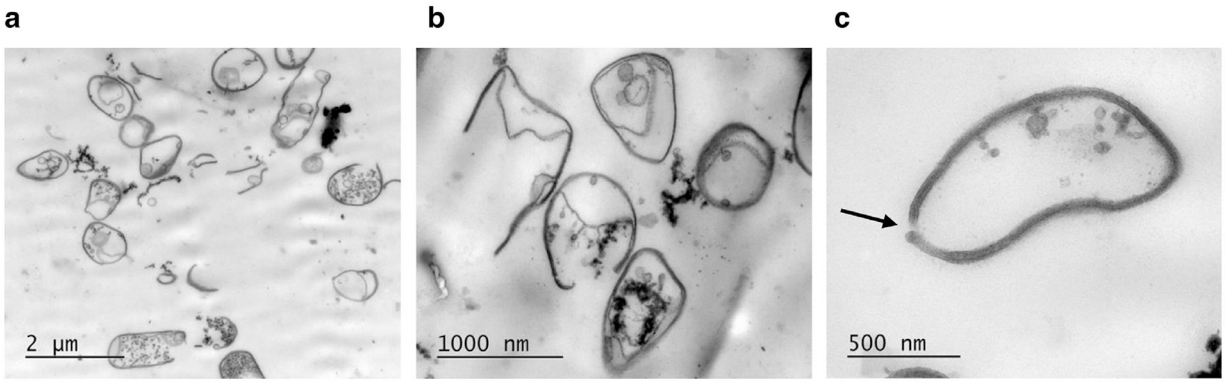


**Fig. 8.**

Transmission electron microscopy appearance of *E. coli* cells from a 5-mL, 20-min exposure treatment combination. At the low magnification (a) (20,000 ×, scale bar is 2 $\mu$m), all cells are damaged, with no signs of cytoplasm visible inside the cells. The cell walls are destroyed, and vesicular bodies are present in the cells. The image is dominated by cellular debris. At the middle magnification (b) (50,000 ×, scale bar is 1 $\mu$m), empty cell walls and fragments populate the optical field. No pili are seen on the surface of the bacteria. At the highest magnification (c) (120,000 ×, scale bar is 500 nm), the arrow points to a 35-nm gap in the wall of a cell nearly devoid of cytoplasm. The surviving fraction associated with thyis treatement combination was 0.004 ± 0.001.


**Fig. 9.**

Transmission electron microscopy appearance of an *E. coli* cells from a 10-mL, 5-min exposure treatment combination. At the low magnification (a) (20,000 ×, scale bar is 2 $\mu$m), the numbers of obviously damaged and apparently intact cells are about the same, with visually intact cells dominating. Similar to unexposed controls (Fig. 6), in cells retaining electron-dense cytoplasm, less dense regions (pili) are associated with the cell wall. Other cells are partially or almost entirely lacking cytoplasm. At the higher magnification (b, c) (40,000 ×, scale bar is 1 $\mu$m), damaged cells have a vacuolated appearance (b); the arrow in (c) points to a region of a cell in which the cell wall has invaginated. The surviving fraction associated with this treatment combination was 0.51 ± 0.16.

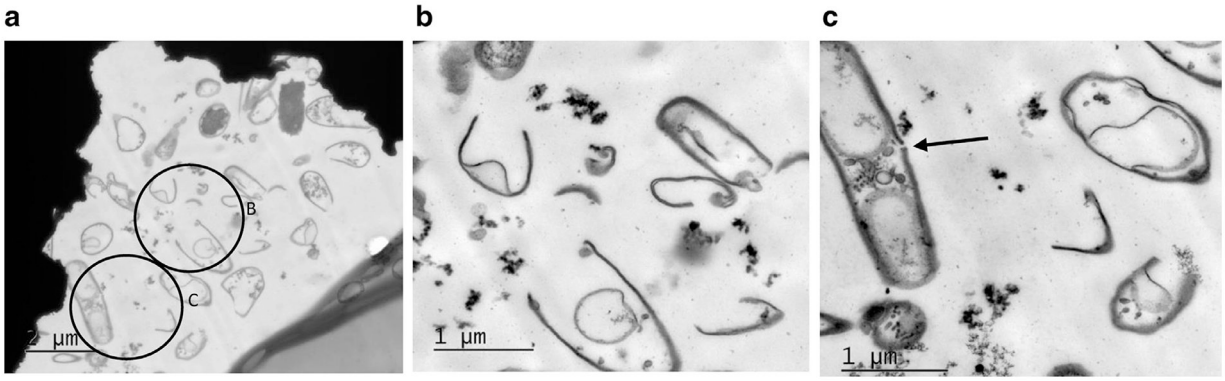


**Fig. 10.**

Transmission electron microscopy appearance of a *E. coli* cells from a 10-mL, 20-min exposure treatment combination. The low magnification image (a) (15,000 ×, scale bar is 2 $\mu$m) shows all cells as evidently damaged. *Circled areas* (b) and (c) are enlarged in the corresponding panels (40,000 ×, scale bar is 1 $\mu$m). The field of view in (b) is populated by cell fragments; cell remnants are essentially devoid of cytoplasm. A mostly intact cell shown in (c) is surrounded by cellular debris. A small gap of approximately 33-nm diameter completely penetrates the cell wall (*arrow*), and a significant amount of cytoplasm appears to have been lost. The surviving fraction associated with this treatment combination was 0.05 ± 0.04.

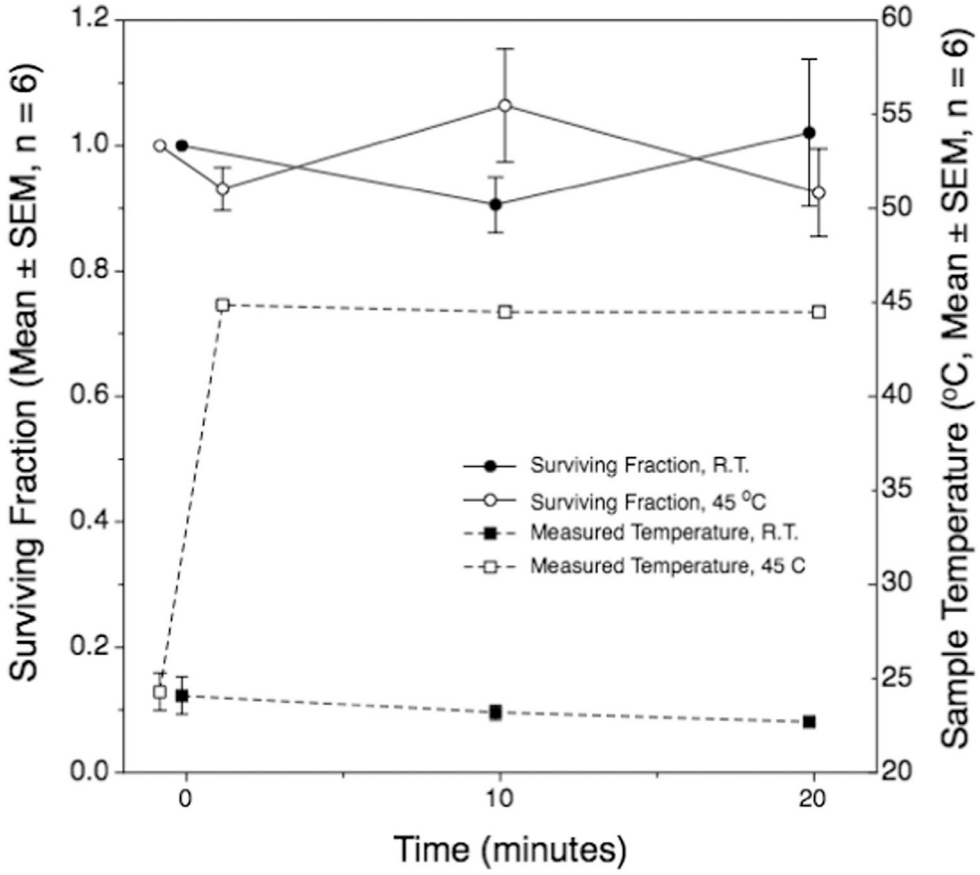


**Fig. 11.**

The surviving fraction of *E. coli* cells incubated in 10-mL polycarbonate vessels for 20 min at either room temperature or 45°C. The temperature history is also illustrated. Heated samples were preheated to 45°C in less than a minute before transfer to the thermally preconditioned polycarbonate vessels. There were no significant differences between any observation and the corresponding initial state. Each point represents the mean of means of six replicate experiments.